ORIGINAL PAPER

Optimized intermolecular potential for nitriles based on Anisotropic United Atoms model

**Mohamed Kamel Hadj-Kali · Vincent Gerbaud ·
Xavier Joulia · Corinne Lacaze-Dufaure ·
Claude Mijoule · Philippe Ungerer**

Abstract An extension of the anisotropic united atoms intermolecular potential model is proposed for nitriles. The electrostatic part of the intermolecular potential is calculated using atomic charges obtained by a simple Mulliken population analysis. The repulsion-dispersion interaction parameters for methyl and methylene groups are taken from transferable AUA4 literature parameters [Ungerer et al., J. Chem. Phys., 2000, 112, 5499]. Non-bonding Lennard-Jones intermolecular potential parameters are regressed for the carbon and nitrogen atoms of the nitrile group (–C≡N) from experimental vapor-liquid equilibrium data of acetonitrile. Gibbs Ensemble Monte Carlo simulations and experimental data agreement is very good for acetonitrile, and better than previous molecular potential proposed by Hloucha et al. [J. Chem. Phys., 2000, 113, 5401]. The transferability of the resulting potential is then successfully tested, without any further readjustment, to predict vapor-liquid phase equilibrium of propionitrile and n-butyronitrile.

M. K. Hadj-Kali (✉) · V. Gerbaud · X. Joulia
Université de Toulouse, Laboratoire de Génie Chimique,
UMR 5503 CNRS – UPS – INPT, BP 1301,
5 Rue Paulin Talabot,
31106 Toulouse Cedex 1, France
e-mail: Mohamed.HadjKali@ensiacet.fr

C. Lacaze-Dufaure · C. Mijoule
Université de Toulouse, Centre Interuniversitaire de Recherche et
d'Ingénierie des Matériaux, UMR 5085 CNRS – UPS – INPT,
118 Rte de Narbonne,
31077 Toulouse Cedex 4, France

P. Ungerer
Institut Français du Pétrole,
1–4 Avenue de Bois Préau,
92852 Rueil-Malmaison Cedex, France

Introduction

Phase equilibrium knowledge is important for the design and the simulation of many separation processes like distillation and extraction. Accuracy of these data is also critical as a 2% error in the evaluation of the vapor-liquid equilibrium of a close boiling mixture like propane - propylene may result in a design error of 30% in the number of stages.

Several engineering and thermodynamic models, like activity coefficient models and equations of state, have been used to generate equilibrium data. However, the use of empirical interaction parameters fitted on existing experimental data within these models reduces their predictive value [1, 2]. This is a serious drawback knowing that just a few tens of thousand phase equilibrium data are recorded in the literature for more than 15 millions of compounds referenced in the Chemical Abstract. Macroscopic predictive thermodynamic models based on chemical group contributions have been proposed [3, 4]. However, their accuracy is unequal unless many subgroups are defined and complexity of use increases [5]. These facts favor the advent of new methods to accurately predict physico-chemical properties.

Among new tools, molecular simulation has emerged as a complementary tool to link the molecular details of a system (atoms masses, energetic interactions, molecules distribution, etc.) to macroscopic properties of experimental interest (physical state, transport coefficients, equilibrium properties, etc.) by means of theoretically significant

statistical thermodynamics concepts. Like real experimentation, molecular simulation basically runs numerical experiments directly on a model system by sampling its configurations upon which properties are averaged and equated to their macroscopic value [6–8]. Besides, molecular simulation can also be knowledge driven in addition to its data driven scope that we investigate in this paper.

The success of molecular simulation for the prediction of accurate thermodynamic properties and for increasing our understanding of complex chemical systems depends on two principal ingredients; namely efficient simulation algorithms to explore the system configurations space and an accurate molecular energy interaction description of the molecular system. Over the years, advances in simulation methods and in computer performance has led to tremendous progress to deal with more and more complex systems, from noble gases, small organic molecules to polymers and biomolecules. The sampling molecular dynamics and Monte Carlo methods have led to histogram reweighting (HR), Gibbs-Duhem integration (GDI) and Gibbs ensemble Monte Carlo (GEMC) techniques to investigate fluid phase equilibrium with great success [9–11]. The GEMC method is used in this paper [8, 12, 13].

A steady effort highlighted by an annual international challenge [14] is set in the world toward better molecular energy interaction description, also called the interaction potential or force field [15], as it is the key challenge for molecular simulation to become a leading technique in getting physico-chemical data with an expected accuracy close to the best experiments. A route consists in using group contributions concepts to derive generic potentials for a small number of chemical groups that could be used to describe many compounds, instead of deriving individual models for all existing compounds.

Involved in this idea, the present work focuses on the development of a set of transferable Lennard-Jones (LJ) parameters for the nitrile group (–C≡N) as an addition to the anisotropic united atoms (AUA) force field parameter set that already contains transferable parameters for linear, branched and cyclic alkanes, olefins, aromatic, ketone and aldehyde molecular fluids [16–21]. Nitriles are industrial solvents and good representatives of polar compounds which phase equilibrium is not trivial to model with macroscopic thermodynamic models [22]: popular cubic equation of states are suited for the investigation of any pressure condition but poorly applied to polar molecules. Activity coefficient models handle polar compounds but are valid only at low pressures. After the optimization of molecules geometry and the computation of atomic charges by a density functional theory method, a methodology similar to the one used by Ungerer et al. [16] is followed. The predictive capacity of the GEMC method coupled with

a suitable interaction model is demonstrated for nitriles in the present work.

The paper outline is as follows. Currently available general force fields for simulations of fluids are reviewed first. Recently developed interaction potentials for phase coexistence properties are described in details along with computational methodologies including both the GEMC method and the LJ parameter optimization method. Our work is then presented: we first performed calculations based on the density functional theory (DFT) to optimize the geometry of acetonitrile, propionitrile and n-butyronitrile and to compute the Mulliken charges. Then, LJ parameters of the (–C≡N) group are optimized on the basis of experimental liquid-vapor equilibrium data of acetonitrile (the reference component). Finally, the successful transferability tests performed on other nitriles (propionitrile and n-butyronitrile) using the optimized parameters without any further adjustment are presented.

Energy interaction potential

The molecular modeling force fields in use today can be interpreted in terms of a summation of the intra and inter molecular forces within the system. Intramolecular forces involve bonded interaction parameters, to calculate bending, stretching and torsion energies and are obtained by fitting to quantum mechanics data. Intermolecular forces sum up in our case to the electrostatic and Van der Waals interactions. Applying population analysis model, partial charges are then used to describe electrostatic interactions: in recent years, the Ewald Summation technique for handling the long range character of the electrostatic interactions has become popular. Van der Waals interaction is described for example by a LJ potential whose parameters are obtained by fitting experimentally observed properties [23].

As a consequence, a great number of intermolecular potential models for fluids have been developed over the past decades, optimized to reproduce the structural and energetic properties of fluids at different operating thermodynamics conditions. As the performance of computers increases, it becomes possible to incorporate more sophisticated models.

Available force fields

Because of their simple chemical structure, non polarity, their abundance in industrial and biological processes and the fact that they can be considered as the aggregation of beads like CH_3, CH_2 or CH, hydrocarbons were the logical starting point for the development of molecular mechanics force field.

All atoms (AA) force fields in which each atom is represented by a separate LJ center are computer intensive and less favored than united atom (UA) potentials pioneered by Jorgensen in 1984 with his OPLS model [24] where hydrogen and carbon atoms within methane, methyl, methylene groups are merged into multi atomic beads. Thus, the number of Van der Waals interactions sites for a given alkane equals its number of carbon atoms and the bead center is located at the carbon atom positions. Other successful UA potentials are the NERD potential [25] proposed by Nath et al. in 1998 or the TraPPE family models [26] developed by Martin and Siepmann.

To account for the intrinsic polarization of the molecules, the mass center can be shifted to as in the anisotropic united atoms (AUA) potential proposed by Toxvaerd for n-alkanes [27], where it is placed between the carbon and the hydrogen atoms of the related group. The first parameter version of this potential (AUA3 parameters) has shown its limitation and has been optimized for n-alkanes by Ungerer et al. in 2000 to obtain a new set of energetic parameters named as AUA4 potential [16] resulting in better predictions of vapor pressures, vaporization enthalpies, liquid densities calculation and the critical temperatures of n-alkanes estimated from coexistence density curves.

AA, UA or AUA models share several common features; in particular, non-bonded dispersion interactions are described by Lennard-Jones 12–6 potential:

$$U^{i,j}(r_{ij}) = 4\varepsilon_{ij}\left[\left(\frac{\sigma_{ij}}{r_{ij}}\right)^{12} - \left(\frac{\sigma_{ij}}{r_{ij}}\right)^{6}\right], \qquad (1)$$

where ε and σ are respectively the LJ energy and diameter parameter. The model developed by Errington and Panagiotopoulos in 1999, considered as a united atom model, uses the Buckingham exponential-6 functional form [28].

Force field transferability

A different approach toward molecular mechanics modeling is the use of a generic force field, meaning that it can be used for a large set of molecules sharing common elementary beads and for the calculation of many properties from transport phenomena coefficients to adsorption coefficients and phase equilibrium [16, 29]. Calculation of different properties using macroscopic models requires different unrelated models, an evidence of the intrinsic genericity of molecular based approaches. The use of a set parameters of elementary chemical beads is an idea that has shown great success at the macroscopic level with the UNIFAC like models, in particular in situations where there are not enough experimental data to parameterize a force field for each given type of molecule because it is risky to interpolate on only a few points.

Transferability of the functional form and parameters is an important feature of a generic force field. Transferability means that the same set of parameters can be used to model a series of related molecules, rather than having to define a new set of parameters for each individual molecule. For example, in order to develop a LJ potential model for nitriles in this work, we will use the set of parameters for all n-alkanes elementary beads (CH_3 and CH_2) and only optimize the parameters relative to the $(-C \equiv N)$ group.

Computational methods

Gibbs ensemble Monte Carlo (GEMC)

The Gibbs ensemble Monte Carlo methodology developed by Panagiotopoulos in 1987 enables direct simulations of phase equilibrium in fluids [10, 12, 13]. Gibbs ensemble simulations are performed in the NVT statistical ensemble on two separate microscopic regions, each within periodic boundary conditions. The thermodynamic requirement for phase coexistence is that each region should be in internal equilibrium, and that temperature, pressure and the chemical potential of all components should be the same in both regions.

System temperature in Monte Carlo simulations is specified in advance. The remaining three conditions are satisfied by performing three types of Monte Carlo moves, displacement of particles within each region to satisfy internal equilibrium, fluctuations in the volume of the two regions to satisfy equality of pressures and transfers of particles between regions to satisfy equality of chemical potentials of all components.

The method has been frequently used in combination with configurational bias sampling technique to improve the sampling of the system configurations and compute phase diagrams of a large number of fluids [8, 30].

The optimization method

The aim of this work, as mentioned above, is the determination of the LJ parameters of the nitrile group $(-C \equiv N)$ for the AUA model, in order to calculate vapor-liquid equilibrium properties of nitrile family of molecules. We followed the optimization method used by Ungerer et al. [16] to optimize the AUA3 potential parameters obtained by Toxvaerd for n-alkanes [27] and applied after by Bourasseau et al. for chemical groups specific to branched and cyclic alkanes [16, 17].

This method allows the optimization of the LJ potential parameters, namely the interaction energy ε and the molecular diameter σ given by Eq. (1), on the basis of three equilibrium properties: liquid density ρ_{liq}, vaporiza-

tion enthalpy ΔH_{vap} and saturation pressure $\ln(P^{sat})$ fitted simultaneously to experimental data using the following dimensionless error criterion:

$$F = \frac{1}{N} \sum_{i}^{N} \frac{\left(X_i^{mod} - X_i^{exp}\right)^2}{S_i^2} \, , \qquad (2)$$

where s_i is the estimated statistical uncertainty on the computed variable X^{mod} and X^{exp} is the associated experimental measurement, either $\ln(P^{sat})$, ΔH_{vap} or ρliq.

When using vaporization enthalpy and liquid density as reference data, a good extrapolation capability toward lower and higher temperatures is expected because these properties control the temperature dependence of the vapor pressure through the Clapeyron equation. Furthermore, density is strongly correlated with other materials properties like mechanical properties, energies of mixing or viscosity/ flow properties. Accurate density prediction suggests that both the shapes of the individual molecules and the intermolecular packing are correctly modeled.

Selecting vapor pressures rather than vapor densities is natural as experimental information is more numerous and consistent for vapor pressure.

Calculations details

Acetonitrile as reference component

The selection of acetonitrile as the reference component has been made in order to focus the contribution of the nitrile group (–C≡N) and to minimize all other undesirable coordination effect. Besides, acetonitrile (methyl cyanide, C_2H_3N) is the nitrile compound for which consistent experimental data are the most abundant [31–35]; spanning both vapor-liquid equilibrium curve and compressed liquid properties for a wide range of temperature and pressure.

Because of its large dipole moment and dielectric constant, acetonitrile is a typical example of a dipolar aprotic liquid, able to dissolve strongly polar and ionic substances.

Simulation of acetonitrile fluid properties has been the subject of many studies. First, Bohm et al. reported a six-site AA model for acetonitrile and showed that it gave an excellent description of the liquid in molecular dynamics simulations [36, 37]. Jorgensen et al. used a three site UA model with a LJ plus Coulomb potential [38] and evaluated a four times decrease in computation time compared with an AA model. They performed NPT Monte Carlo simulations at two temperatures (298.15 K and 343.15 K) and atmospheric pressure. Liquid properties, such as density and heat of vaporization agreed within 2 per cent with experimental values. In addition, they emphasize the

importance of electrostatic interactions in determining the liquid structure.

Recently, Hloucha et al. performed a comprehensive study in an attempt to bridge the gap between *ab initio* interaction energy information and macroscopic properties prediction [39, 40]. In their second publication, they performed molecular simulation calculations using the accurate potential based on the *ab initio* work of Bukowski et al. [41] who applied symmetry adapted perturbation theory (SAPT) to compute interaction energies for many hundreds of configurations of pairs of molecules, including the acetonitrile-acetonitrile pair. As described in their original paper, Hloucha et al. performed three different fits for the *ab initio* acetonitrile pair interaction energies obtained by Bukowski et al. to the well known LJ potential (their named ACN1 and ACN2 models) and modified Buckingham (ACN3 model) plus Coulomb site-site potentials. These potentials were then used in Gibbs ensemble Monte Carlo simulations to calculate the phase diagram of acetonitrile. It was found that the phase behavior prediction is highly dependent on the details of the interaction potentials developed, the ACN1 model giving the best equilibrium curve prediction.

Apart from correlations in databases like DIPPR [42], a Russian article [31] provides experimental data for a wide range of temperature and pressure values for two other nitriles: propionitrile and n-butyronitrile molecules. Thus, the evident choice of our reference component was the acetonitrile molecule on which the LJ potential parameters will be optimized and their transferability will be tested for both propionitrile and n-butyronitrile.

Preliminary calculations

Electrostatic interaction

DFT calculations were performed to determine the most stable conformation and the charge distribution on acetonitrile, propionitrile and n-butyronitrile molecules.

We used the deMon program package [43, 44] with VWN local potential [45] and non-local gradient based corrections of Perdew and Perdew et al. [46–48] for the exchange and correlation terms. For the carbon and nitrogen atoms we used the (7111/411/1*) orbital basis sets and the corresponding (5,2; 5,2) auxiliary basis set. The hydrogen atoms were treated with the (41/1*) orbital basis set and (4,2; 4,2) auxiliary basis set.

A full geometry optimization was performed using a conjugate gradient method for each molecule. We performed polarized calculations and the systems were taken in their more stable spin state (singlet).

Bond length and angle values for the optimized geometry of each molecule are reported in Figs. 1, 2 and 3 respectively
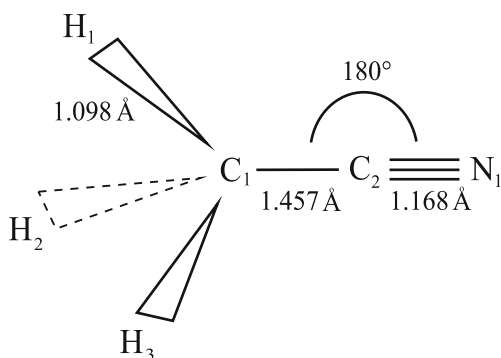
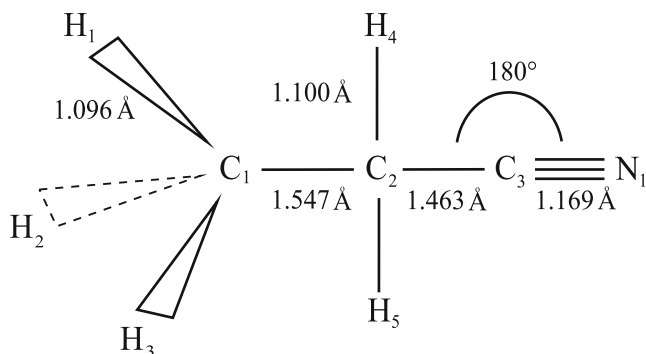**Fig. 1** Schematic representation of acetonitrile

for acetonitrile, propionitrile and n-butyronitrile. For aceto-
nitrile and propionitrile, Tables 1 and 2 show a comparison
between our results and experimental counterpart values
cited by Goldstein et al. [49] who also performed molecular
mechanics calculations with MM3 force field for nitrile
molecules reported in these tables. In addition, and only for
acetonitrile, the resulting geometry is compared to *ab initio*
calculations performed by Williams et al. [50].

The charge distribution on the three nitrile molecules
was determined by a Mulliken population analysis (Table 3).
The net charge on the nitrogen and the carbon atoms of the
nitrile group are similar for the three molecules, showing
the consistency of the Mulliken analysis performed even if,
as known, these charges depend largely on the basis set and
do not reproduce correctly the electrostatic potentials
around the molecules. In addition, calculated dipolar
moment agrees well with experiment.

Intramolecular interactions

We considered nitriles as semiflexible chain molecules with
a rigid nitrile group ($-C \equiv N$). The flexibility of the alkane
chain is taken into account by a harmonic bending
potential, function of the bond angle θ around an
equilibrium value θ_0 by an expression of the form:

$$U^{bend}(\theta) = \frac{1}{2} k_\theta (\cos\theta - \cos\theta_0)^2 . \qquad (3)$$

Fig. 2 Schematic representation of propionitrile
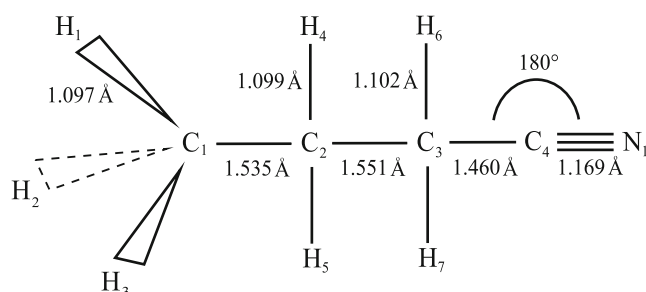
Fig. 3 Schematic representation of n-butyronitrile

Whereas, the torsion potential taken into account only
for n-butyronitrile is of the form:

$$U^{tors}(\phi) = \sum_{j=0}^{8} a_j \cos^j(\phi) , \qquad (4)$$

where φ is the dihedral angle.

Intramolecular parameters are taken from the literature
[16, 49, 51] and given in Table 4.

No bonded van der Waals interactions between united
atoms belonging to the same molecule and separated by
more than three chemical bonds are also included and
modeled by LJ centers of force.

Simulation details

In order to compute phase equilibrium, we used the GEMC
method. Every phase in the system was represented by a
cubic simulation box using periodic boundary conditions to
avoid boundary effects. Simulations have been performed
with a total number of 200 molecules. The occurrences for
the various types of moves were taken equal to 10%
for translations, rotations and internal relaxation, 0.5% for
volume changes and 69.5% for transfers. We used standard
long-range corrections, associated with a cutoff radius equal
to the half of the simulation box length. The simulation
length was 5.10^6 iterations for acetonitrile and was
extended when we tested the parameter transferability to

Table 1 Comparison between computed and experimental geometries
of acetonitrile

Distance (Å)	Exp	ab initio[a]	MM3[b]	DFT[c]
C_1—C_2	1.468	1.478	1.470	1.457 (- 0.75%)
C_1—$H_{1,2,3}$	1.095	1.099	1.108	1.098 (+0.27%)
$C_2 \equiv N_1$	1.159	1.171	1.158	1.168 (+0.77%)
Angles (deg)	Exp	ab initio[a]	MM3[a]	DFT[b]
C_2—C_1—H	109.7	109.7	110.0	110.3 (+0.55%)
H—C_1—H	108.9	109.2	108.9	108.6 (- 0.25%)
C_1—$C_2 \equiv N$	————	180.0	180.0	179.8

[a] Williams et al. 50 [b] Goldstein et al. 49 [c] This work

Table 2 Comparison of computed propionitrile molecular geometry with both experimental data cited by Goldstein et al. [49] and his molecular mechanics calculation

Distance (Å)	Exp	MM3[a]	DFT[b]
C_1—C_2	1.548	1.533	1.547 (-0.06%)
C_2—C_3	1.474	1.473	1.463 (-0.74%)
C_1—H	————	1.110	1.096
C_2—H	1.091	1.113	1.096 (+0.46%)
$C_3 \equiv N_1$	1.157	1.158	1.169 (+0.77%)
Angles (deg)	Exp	MM3[a]	DFT[b]
C_1—C_2—C_3	110.3	110.5	112.48 (+1.97%)
C_3—C_2—$H_{4,5}$	109.3	108.15	
C_1—C_2—$H_{4,5}$	————	110.0	110.70
C_2—C_1—$H_{1,2,3}$	————	111.5	110.58
H_4—C_2—H_5	109.2	107.3	106.38 (-2.58%)
C_2—$C_3 \equiv N$	————	180.0	178.93

[a] Goldstein et al. [49]   [b] This work

8.10^6 for propionitrile and 9.10^6 for n-butyronitrile to better explore the configuration space for longer molecules.

The desired equilibrium properties were computed by averaging after a stabilization step of 1.10^6 iterations. Vapor pressure was taken as the average pressure in the vapor simulation box. The molar vaporization enthalpy was simply computed as the difference between the average molar enthalpies of the liquid and vapor simulation boxes, and finally, the average liquid density was determined directly as the ratio of the average mass of the liquid simulation box and its volume.

Statistical uncertainties for $\ln(P^{sat})$, ΔH_{vap} and ρ_{liq} were respectively 5%, 2% and 0.5% in the favorable range of reduced temperatures for the GEMC Method ($0.60 < T/Tc < 0.95$), i.e., far from both high temperatures (the critical region) and low temperatures where the GEMC method

Table 3 Atomic charges for acetonitrile, propionitrile and n-butyronitrile based on Mulliken population analysis (electrons)

	acetonitrile	propionitrile	n-butyronitrile
C_1	-0.40	-0.31	-0.33
C_2	+0.15	-0.25	-0.16
C_3	—	+0.13	-0.25
C_4	—	—	+0.12
H_1	+0.16	+0.12	+0.11
H_2	+0.16	+0.12	+0.11
H_3	+0.16	+0.12	+0.11
H_4	—	+0.15	+0.12
H_5	—	+0.15	+0.12
H_6	—	—	+0.14
H_7	—	—	+0.14
N_1	-0.23	-0.23	-0.23
μ/D cal.	4.01	4.09	4.21
μ/D exp.	3.93	4.02	4.07

Table 4 Molecular weight, equilibrium angles, bending force constants and torsion potential parameters

Molecular weight (g/mol)	CH_3		15.030
	CH_2		14.030
	C $_{(C \equiv N)}$		12.011
	N $_{(C \equiv N)}$		14.006
Bending	— C — C — C —	θ_0 (deg)	112.0[a]
		k_{bend} (K)	74 900[a]
	— C — C — C $\equiv$	θ_0 (deg)	108.8[b]
		k_{bend} (K)	69 500[b]
	— C — C $\equiv$ N	θ_0 (deg)	180.0[b]
		k_{bend} (K)	24 300[b]
Torsion	— C — CH_2 — CH_2 — C	a_0 (K)	1 001.35[c]
		a_1 (K)	2 129.52[c]
		a_2 (K)	-303.06[c]
		a_3 (K)	-3 612.27[c]
		a_4 (K)	2 226.71[c]
		a_5 (K)	1 965.93[c]
		a_6 (K)	-4 489.34[c]
		a_7 (K)	-1 736.22[c]
		a_8 (K)	2 817.37[c]

[a] Ungerer et al. [16]   [b] Goldstein et al. [49]   [c] Toxvaerd [51]

shows a low rate of transfer between the liquid and the vapor box [8].

The critical properties are estimated by fitting the subcritical simulation data to the density scaling law for the critical temperature T_c:

$$\rho_{liq} - \rho_{vap} = B(T - T_c)^\beta , \qquad (5)$$

and to the law of rectilinear diameters for the critical density ρ_c:

$$\frac{\rho_{liq} + \rho_{vap}}{2} = \rho_c + A(T - T_c) , \qquad (6)$$

where ρ_{liq} and ρ_{vap} are the coexisting densities of the liquid phase and the vapor phase at a given temperature T, A and B are fitting parameters and the critical exponent β is taken equal to 0.325 [8].

Inilization step

The reference component (acetonitrile) is decomposed into three force centers: the CH_3 group described by AUA4 parameters already obtained by Ungerer et al. [16] given in Table 5 and the carbon and nitrogen atoms whose LJ energetic parameters are optimized in this work. The same decomposition was taken for the other nitriles with the introduction of literature AUA4 parameters of the CH_2 group [16] also given in Table 5.

Table 5 CH_2 and CH_3 LJ parameters of AUA4 potential taken from Ungerer et al. [16]

	σ (Å)	ε/kB (K)	δ (Å)
CH_3	3.6072	120.15	0.21584
CH_2	3.4612	86.29	0.38405

To calculate the LJ parameters for unlike groups (or atoms such as nitrogen) interactions, Lorentz-Berthelot combining rules are employed:

$$\varepsilon_{ij} = \sqrt{\varepsilon_{ii}\varepsilon_{jj}} \quad \sigma_{ij} = \frac{\sigma_{ii} + \sigma_{jj}}{2} . \tag{7}$$

The selected LJ parameters were optimized on the basis of experimental equilibrium data of acetonitrile at three different temperatures (433.15 K, 443.15 K and 453.15 K). As described in the literature [16], we perform GEMC simulations at these temperatures in order to minimize the dimensionless error function F given by Eq. (2) considered, here, as a function of four parameters, namely the two interaction energies of carbon and nitrogen atoms ε_C, ε_N and their molecular diameters σ_C, σ_N, with s_i taken equal to 0.1 for ln(Psat), 1 kJ mol^{-1} for vaporization enthalpy and 10 kg/m^3 for the molecular density.

LJ parameters values are initialized on the basis of preliminary calculations of vapor-liquid coexistence curve of acetonitrile (ε_C/k_B= 100.0K, ε_N/k_B= 140.0K, σ_C= 3.30A, σ_N= 3.35A). This set of parameters enables just the GEMC to provide the separation of the two phases at one given temperature (433.15 K). Table 6 displays the optimized energetic parameters obtained after two iterations.

With the optimized LJ parameter values (Tables 5 and 6), GEMC simulations at different temperatures were performed for acetonitrile. Figure 4 plots the variation of the temperature versus the density in the two phases. We compared our values (triangle up) with both experimental data obtained by Francesconi et al. [32] presented by circles and those provided by Warowny [35] (cross symbol). We can see that simulation points show a good agreement with experimental data.

Figure 5 plots the vapor pressure dependence of acetonitrile over the temperature. Our results are close to the experimental data of both Warowny [35] and Chakhmuradov

Table 6 Optimized LJ parameters

| C (C ≡ N)		N (C ≡ N)	
ε/k_B (K)	σ (Å)	ε/k_B (K)	σ (Å)
95.52	3.218	162.41	3.564
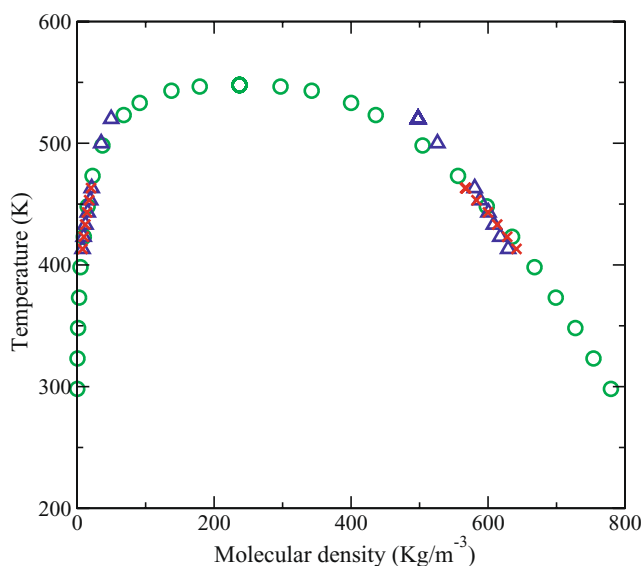
Fig. 4 Vapor-liquid coexistence curve of acetonitrile given the equilibrium temperature versus the molecular density obtained in this work (triangles) compared with experimental data of Francesconi et al. [32] (circles) and Warowny [35] (cross symbols)

et al. [31] and better than previous simulation results obtained in 2000 by Hloucha et al. [40]. Figure 6 gives simulated enthalpy of vaporization compared with DIPPR data.

Transferability test

As mentioned earlier, two important issues, highlighting the solid basis of one developed force field and its prediction
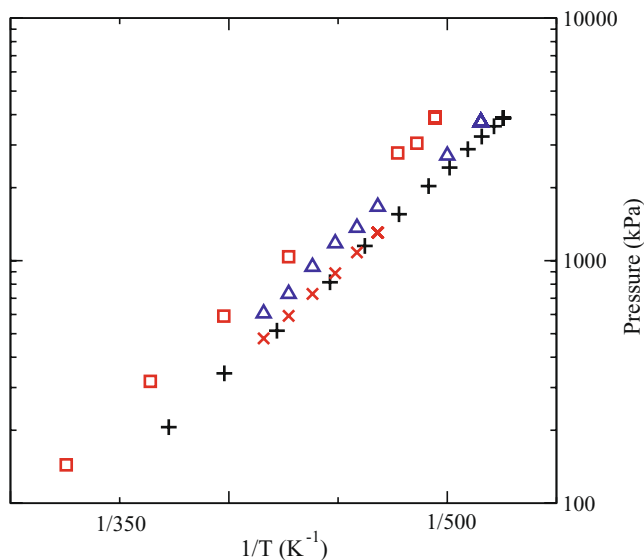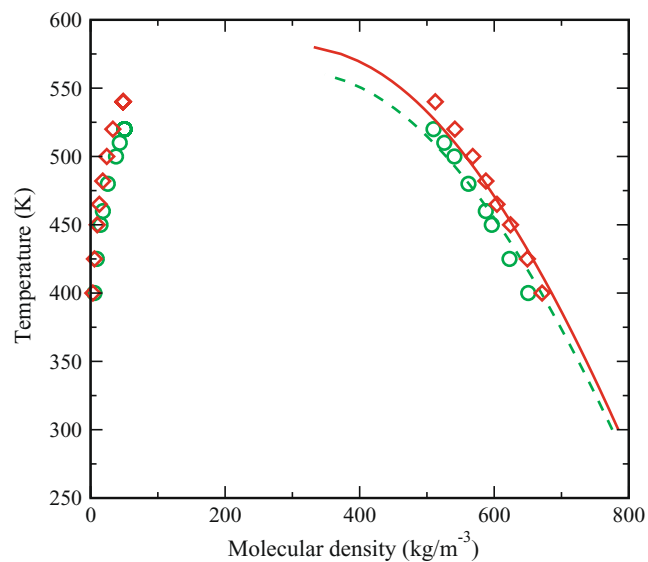

Fig. 5 Vapor pressure of acetonitrile obtained in this work (triangles) compared with both experimental datas (of Charmuradov [31] (plus symbols) and Warowny [35] (cross symbols)) and previous simulated data obtained earlier by Hloucha et al. [40] (squares)
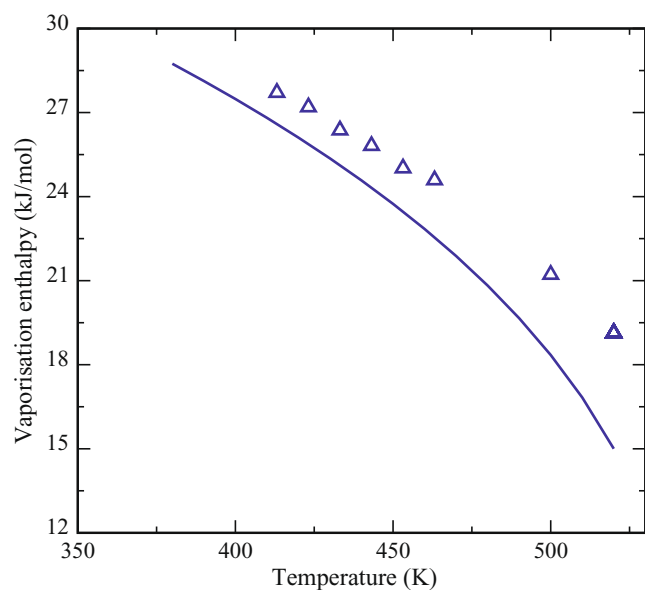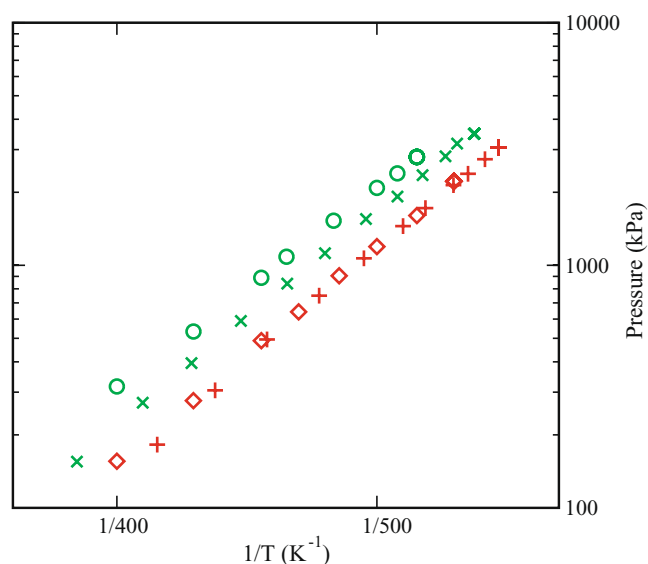
Fig. 6 Calculated vaporization enthalpies of acetonitrile (triangles) compared with DIPPR data (solid line)

Fig. 8 Vapor pressure of both propionitrile (circles) and n-butyronitrile (diamonds) compared with experimental datas of Charmuradov 31 (cross symbols for propionitrile and plus symbols for n-butyronitrile)

potentialities, are its transferability and its ability to predict properties at state points far from experimental data. Transferability of our optimized parameters is tested for propionitrile and n-butyronitrile: $(-C \equiv N)$ LJ parameters are taken from the acetonitrile set. CH_3 and CH_2 parameters are taken from the literature [16] as well as intramolecular parameters [16, 51] (Tables 4 and 5). Only electrostatic interaction parameters (Table 3) and geometry parameters (Figs. 2 and 3) are readjusted for propionitrile and n-butyronitrile. Results are compared with both DIPPR data
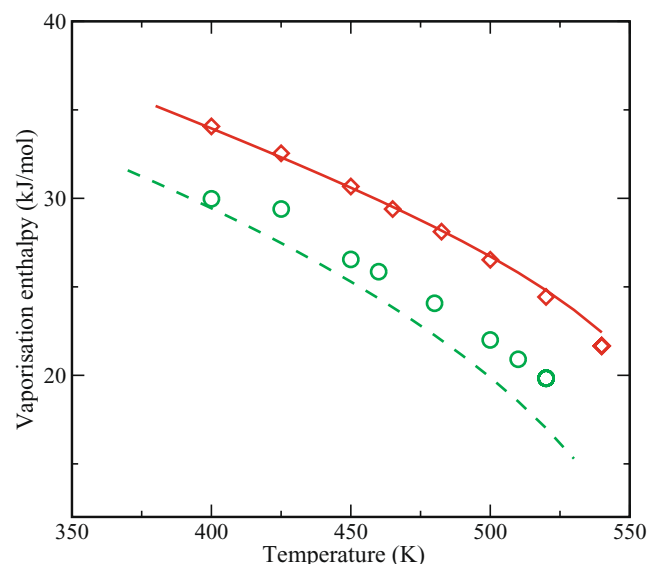
in Fig. 7 for density versus temperature and experimental data of Charmuradov et al. [31] in Fig. 8 for saturated pressure versus temperature. Variation of the vaporization enthalpy versus the temperature is compared with DIPPR data in Fig. 9 for the two molecules. Agreement is satisfactory and even quite remarkable for n-butyronitrile.

Finally, the estimated critical densities and temperatures for the three molecules are given in Table 7. These values are estimated to be within 1 to 6% of the experimental data.

Fig. 7 Obtained vapor-liquid coexistence curves of both propionitrile (circles) and n-butyronitrile (diamonds) given the equilibrium temperature versus the molecular density compared with DIPPR correlations (dashed lines for propionitrile and solid lines for n-butyronitrile)

Fig. 9 Enthalpies of vaporization of propionitrile (circles) and n-butronitrile (diamonds) compared with DIPPR data (dashed lines for propionitrile and solid lines for n-butyronitrile)

Table 7 Estimated critical points for acetonitrile, propionitrile and n-butyronitrile

Compound	Critical temperature /K		Critical density/kg.m^{-3}	
	Exp[a]	Sim	Exp[a]	Sim
Acetonitrile	547.85	582.54	237.10	247.36
Propionitrile	564.40	586.29	240.52	254.35
n-butyronitrile	582.85	609.17	248.80	250.96

Discussion

Comparison between the $(-C \equiv N)$ σ and ε LJ parameters and AUA4 force field LJ parameters for alkane and alkene chemical groups CH_4, CH_3, CH_2, CH and $C(C=C)$ is shown in Figs. 10 and 11. The $(-C \equiv N)$ LJ energetic parameters are consistent with the other AUA4 parameters.

Considering the $C_{(-C \equiv N)}$ atom, it is involved in two chemical bonds with C and N. From Figs. 1 to 3, the $-C-C_{(-C \equiv N)}$ bond length, around 1.465 Å, is closer to C-C single bond length rather than to C=C or $C \equiv C$ multiple bond length. However, the $(-C \equiv N)$ bond length is significantly shorter around 1.168 Å.

Consistently, the $\sigma_{C(-C \equiv N)}$ LJ parameter lies between that of the –C and of the =C (Fig. 10). The $\sigma_{N(-C \equiv N)}$ LJ parameter is greater, in accordance with the terminal position of this atom in the nitrile chemical group as σ representing the diameter at which the LJ potential nullifies, it is likely that for a terminal atom, a fortiori with a significant electronegative one like nitrogen, this value is greater than for LJ centers located inside the molecule, like CH_2 and CH.
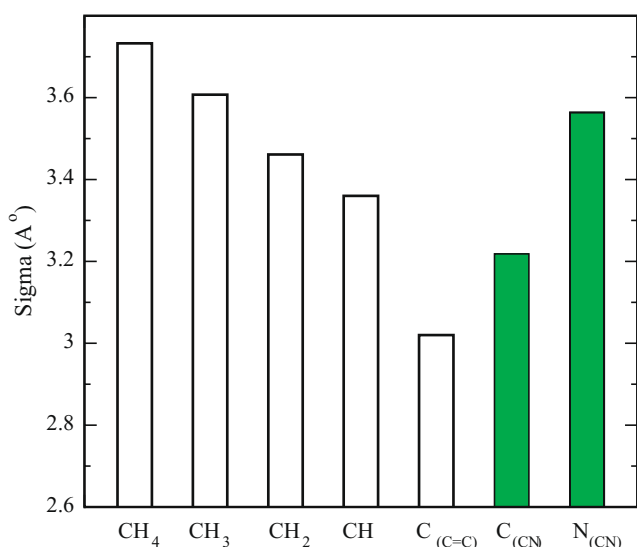
Fig. 10 Molecular diameter parameter for the LJ potential (σ) of the carbon and nitrogen atoms of the nitrile group $(-C \equiv N)$ compared with AUA4 force field linear and branched alkanes parameters
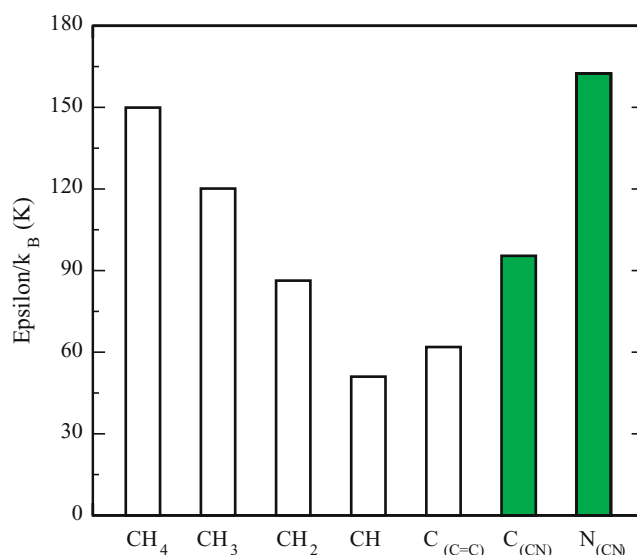
Fig. 11 Energetic parameter for the LJ potential (ε/k_B) of the carbon and nitrogen atoms of the nitrile group $(-C \equiv N)$ compared with AUA4 force field linear and branched alkanes parameters

The ε LJ parameter is the depth of the LJ potential, in other words, its interaction energy strength. For nitrogen, more electronegative than carbon or hydrogen, we note that the optimized $\varepsilon_{N(-C \equiv N)}$ LJ parameter is greater that any ε_C value (Fig. 11). The $\varepsilon_{C(-C \equiv N)}$ LJ parameter is comparable to the value for the CH_2 group. Electronegativity influence is also perceived in the negative partial charge of the nitrogen atom (Table 3).

As already observed in the literature, the critical temperature calculated for the three nitriles using Eqs. 5 and 6 is overestimated by more than 20 K, a value that is larger than commonly accepted uncertainty of the critical point values but within 6% of the experimental value. On the other hand, the critical density agrees better with the experimental data.

Conclusions

A methodology to derive and to optimize the parameters of a transferable potential was applied in this paper to nitriles within the AUA4 force field. The electrostatic potential part of the potential was modeled by coulomb potential using partial charges obtained by a Mulliken population analysis. The repulsion–dispersion part was modeled by anisotropic Lennard-Jones sites. LJ parameters for methyl and ethyl groups were taken from a previous AUA4 study on alkanes [16] and AUA4 σ and ε LJ parameters for the remaining carbon and nitrogen atoms of the nitrile groups were fitted to vapor-liquid equilibrium experimental data of acetonitrile. Consistent with other AUA4 LJ parameters, they were

proven to be transferable as they yield good prediction of the vapor-liquid equilibrium of both propionitrile and n-butyronitrile.

References

1. Prausnitz JM, Lichtenthaler RN and de Azevedo EG (1999) Molecular thermodynamics of fluid-phase equilibria. 3rd edn. Prentice- Hall, Upper Saddle River, NJ ISBN 0-13-977745-8
2. Prausnitz JM, Tavares FW (2004) AIChE J 50(4):739–761
3. Hansen HK, Schiller M, Fredenslund A, Gmehling J, Rasmussen P (1991) Ind Eng Chem Res 5(30):2352–2355
4. Horstmann S, Fischer K, Gmehling J (2000) Fluid Phase Equilibria 167:173–186
5. Gani R, Constantinou L (1996) Fluid Phase Equilibria. 116 (1–2):75–86
6. Allen MP, Tildesley DJ (1987) Computer simulation of liquids. Oxford Science, ISBN 0-19-855645-4
7. McQuarrie DA (1976) Statistical Mechanics, Harper Collins Publishers, New york, ISBN 06-044366-9
8. Frenkel D, Smit B (1996) Understanding molecular simulation from algorithms to applications. Academic, San Diego, ISBN 0-12-267370-0
9. Kofke DA (1993) Mol Phys 78:1331–1336
10. Panagiotopoulos AZ (2000) J Phys Cond Matter 12:R25–R52
11. De Pablo JJ, Escobedo FA (2002) AIChE 48(12):2716–2721
12. Panagiotopoulos AZ (1987) Mol. Phys. 61:813–826
13. Panagiotopoulos AZ Quirke N, Stapleton M, Tildesley D (1988) J Mol Phys 63(4):527–545
14. Case F, Chaka A, Friend DG, Frurip D Golab J, Johnson R, Moore J, Mountain RD, Olson J, Schiller M, Storer J (2004) Fluid Phase Equilibria 217(1):1–10
15. Panagiotopoulos AZ (2001) AIChE Symp Ser No 325, 97:61–70
16. Ungerer P, Beauvais C, Delhommelle J, Boutin A, Rousseau B, Fuchs AH (2000) J Chem Phys 112(12):5499–5510
17. Bourasseau E, Ungerer P, Boutin A, Fuchs AH (2002) Mol Sim 28(4):317–336
18. Bourasseau E, Ungerer P, Boutin A (2002) J Phys Chem B 106:5483–5491
19. Bourasseau E, Haboudou M, Boutin A, Fuchs AH, Ungerer P (2003) J Chem Phys 118:3020–3034
20. Ahunbay MG, Perez-Pellitero J, Contreras-Camacho RO, Teuler JM, Ungerer P, Mackie AD, Lachet V (2005) J Phys Chem B 109 (7):2970–2976
21. Kranias S, Pattou D, Lévy B, Boutin A (2003) Phys Chem Chem Phys 5:4175–4179
22. Vidal J, (2003) Thermodynamics: Applications in Chemical Engineering and the Petroleum Industry, Editions Technip, ISBN 2710808005
23. Leach AR (1996) Molecular Modelling. Addison- Wesley, Boston, ISBN 0-582-23933-8
24. Jorgensen WL, Madura JD, Swenson CJ (1984) J Am Chem Soc 106:6638–6646
25. Nath SK, Escobedo FA, de Pablo JJ (1998) J Chem Phys 108:9905–9911
26. Martin MG, Siepmann I (1998) J Phys Chem B 102:2569–2577
27. Toxvaerd S (1990) J Chem Phys 93:4290–4295
28. Errington JR, Panagiotopoulos AZ (1999) J Phys Chem B 103:6314–6322
29. Nieto-Draghi C, Ungerer P, Rousseau B (2006) J Chem Phys 125 (4):044517(1–15)
30. Smit B, Karaboni S, Siepmann I (1995) J Chem Phys 102 (5):2126–2140
31. Chakhmuradov CG, Guseinov SO (1984) Phys Chem (Iz Vys Uc Zav) 65–69 (in Russian)
32. Francesconi AZ, Franck EU, Lentz H (1975) Ber Bunsen-Ges 79:897–901 (in German)
33. Kratzke H, Müller S (1985) J Chem Therm 17:151–158
34. Mousa AHN (1981) J Chem Therms 13:201–202
35. Warowny WJ (1994) Chem Eng Data 39:275–280
36. Bohm HJ, McDonald IR, Madden PA (1983) Mol Phys 49:347–360
37. Bohm HJ, Lynden-Bell RM, Madden PA, McDonald IR (1984) Mol Phys 51:761–777
38. Jorgensen WL, Briggs JM (1988) Mol Phys 63(4):547–558
39. Hloucha M, Deiters UK (1997) Mol Phys 90(4):593–597
40. Hloucha M, Sum AK, Sandler SI (2000) J Chem Phys 113 (13):5401–5406
41. Bukowski R, Szalewicz K, Chabalowski CF (1999) J Phys Chem A 103:7322–7340
42. AIChE Design Institute for Physical Property Project, Property estimation handbook (1987) American Institute of Chemical Engineers
43. St-Amant A, Salahub DR (1990) Chem Phys Letters 169:387–392
44. St-Amant A (1992) Dissertation, Montréal University
45. Vosko SH, Wilk L, Nusair M (1980) Can J Phys 58:1200–1211
46. Perdew JP (1985) Phys Rev Letters 55:1665–1668
47. Perdew JP, Wang Y (1986) Phys Rev B 33:8800–8810
48. Perdew JP (1986) Phys Rev B 33:8822–8825
49. Goldstein E, Buyong MA, Lii JH, Allinger NL (1996) J Phys Org Chem 9:191–202
50. Williams HL, Rice BM, Chabalowski CF (1998) J Phys Chem A 102:6981–6992
51. Toxvaerd S (1997) J Chem Phys 107:5197–5204